Conclusive evidence of abrupt coagulation inside the void during cyclic nanoparticle formation in reactive plasma

AIP | Applied Physics Letters

Conclusive evidence of abrupt coagulation inside the void during cyclic nanoparticle formation in reactive plasma

F. M. J. H. van de Wetering, S. Nijdam, and J. Beckers

Citation: Applied Physics Letters **109**, 043105 (2016); doi: 10.1063/1.4959835
View online: http://dx.doi.org/10.1063/1.4959835
View Table of Contents: http://scitation.aip.org/content/aip/journal/apl/109/4?ver=pdfcov
Published by the AIP Publishing

Conclusive evidence of abrupt coagulation inside the void during cyclic nanoparticle formation in reactive plasma

F. M. J. H. van de Wetering, S. Nijdam, and J. Beckers
Eindhoven University of Technology, P.O. Box 513, 5600 MB Eindhoven, The Netherlands

(Received 28 May 2016; accepted 14 July 2016; published online 25 July 2016)

In this letter, we present scanning electron microscopy (SEM) results that confirm in a direct way our earlier explanation of an abrupt coagulation event as the cause for the void hiccup. In a recent paper, we reported on the fast and interrupted expansion of voids in a reactive dusty argon–acetylene plasma. The voids appeared one after the other, each showing a peculiar, though reproducible, behavior of successive periods of fast expansion, abrupt contraction, and continued expansion. The abrupt contraction was termed "hiccup" and was related to collective coagulation of a new generation of nanoparticles growing in the void using relatively indirect methods: electron density measurements and optical emission spectroscopy. In this letter, we present conclusive evidence using SEM of particles collected at different moments in time spanning several growth cycles, which enables us to follow the nanoparticle formation process in great detail. *Published by AIP Publishing.* [http://dx.doi.org/10.1063/1.4959835]

Reactive plasmas are able to grow nanoparticles in the plasma volume by polymerization of a suitable reactive gas. The resulting clusters can subsequently grow to particles several hundreds of nanometers in size.[1] Reactive dusty plasmas are studied with the aim to produce nanoparticles in a controlled way and to use the particles as building blocks for further applications, such as nanocomposites, biomimetic surfaces, and quantum dots.[2–4] Furthermore, the spontaneous formation of nanoparticles in the plasma volume of industrial plasma applications is often an unwanted side effect, where reactive gases are for example used in etching plasmas or for the production of thin photosensitive films for solar cell applications.[5,6] Nanoparticles also present challenges in for example the semiconductor industry (photolithography) and in fusion reactors.[7–9] It is therefore essential that the nanoparticle formation processes are understood and can be controlled or suppressed if necessary.

Spontaneous polymerization of feed gas molecules and subsequent homogeneous nucleation is the first step in the formation of nanoparticles in reactive plasmas and produces nanometer-sized clusters.[10–14] Abrupt coagulation follows when a critical cluster density is reached, pushing protoparticles together and "fusing" them, provided they are not electrostatically repelling each other. Since, in a plasma, electrons have a much higher velocity than ions, particles with diameters of some tens of nanometers quickly attain a permanent negative net charge. Consequently, further coagulation stops and the nanoparticles are trapped (confined) in the plasma. During this phase, the free-electron density drops and electron energy increases in the vicinity of the nanoparticles. The last step is a continuous growth of the particles due to the accretion of ions and radicals from the plasma.

Due to the mutual Coulomb repulsion between the negatively charged grains and the confining ambipolar electric field, a dense nanoparticle cloud usually forms that almost completely fills the plasma volume. In our discharge geometry, dust particles predominantly reside in the bulk of the plasma, see the laser light scattering results presented previously (Figures 5 and 6 of that publication).[15] However, bigger and heavier particles are pulled/pushed downward due to gravity and gas flow and they will probably penetrate deeper into the sheath areas, where the electric field is high enough to confine them. A frequent observation is the formation of a macroscopic region inside the dust cloud that is free of coagulated particles.[16–20] This region is termed the dust void. It results (mainly) from the interplay between the ion drag force (momentum transfer between flowing ions and nanoparticles) that pushes particles away from the plasma center and the confining ambipolar electric field.[21] The plasma (electron density/energy, resulting optical emission) can differ drastically between the void and dusty region surrounding it.[20,22–24] For example, the electron density is generally higher inside the void due to the absence of the substantial electron sink that big (coagulated) nanoparticles present.

In a recent paper,[15] we reported on the fast and interrupted expansion of voids in a reactive dusty argon–acetylene plasma. The voids appeared successively and each void showed periods of steady expansion, fast expansion, abrupt contraction, and continued expansion. We call this surprising abrupt contraction "hiccup" and we related it to collective coagulation of a new generation of nanoparticles forming in the void. This conclusion was supported by optical emission spectroscopy (OES) and electron density measurements both inside and outside the void. The electron density was determined with non-intrusive microwave cavity resonance spectroscopy (MCRS), using two resonant modes with different spatial weighting. In this letter, we present the results of scanning electron microscopy (SEM) of nanoparticles collected at different moments in time spanning several growth cycles, allowing us to follow the nanoparticle formation process directly and in great detail. As will be shown, the SEM results show conclusively that an abrupt coagulation event indeed causes the void hiccup.

The experimental setup is described in detail in the previous paper.[15] The discharge parameters are as follows. Gas

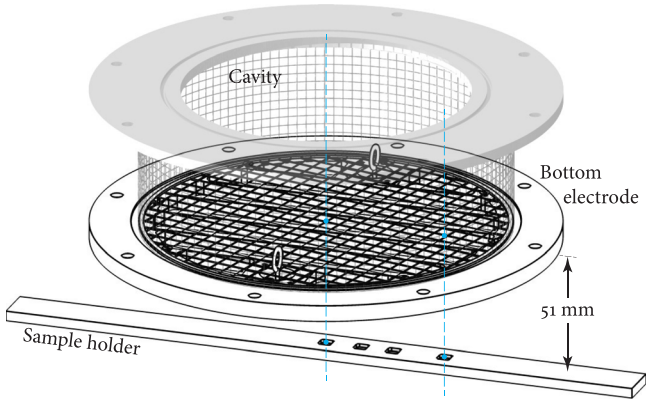

FIG. 1. The bottom electrode of the discharge chamber with the sample holder in place. The sample holder is a perspex strip containing four trenches in which small silicon wafers can be placed. One of the trenches is directly below the center of the discharge chamber. The discharge chamber also serves as microwave cavity and its side wall and top plate are shown as well (translucent). Mesh sizes are exaggerated for clarity.

pressure: 10 Pa, argon flow rate: 17.4 sccm, acetylene flow rate: 2.3 sccm, and plasma-dissipated power: about 19 W, which is coupled capacitively at an RF frequency of 13.56 MHz. The size (distribution) of the nanoparticles growing in time is determined with SEM analysis. To this end, several dusty plasmas are run successively under the same experimental conditions. A perspex sample holder is placed 51 mm below the bottom electrode. This electrode mainly consists of a circular metal mesh (thread width 0.35 mm, mesh size 1.06 mm). Small ($\sim$0.25 cm^2) silicon wafers are placed in 1.5 mm deep 6 mm $\times$ 6 mm wide trenches in the sample holder. One of the trenches is directly below the center of the discharge chamber, whereas the outermost trench is close to the edge of the discharge chamber, see Figure 1. Since the bottom electrode and side wall of our discharge chamber are made of a mesh, particles can relatively freely leave the discharge chamber. However, during their growth in the plasma, particles will not leave it as long as confining forces (mostly the ambipolar electric field working on the negatively charged grains) exceed forces pushing particles outward (e.g., gravity and neutral/ion drag). Particles will fall *en masse* when the power is switched off. The runs differ solely in the time at which the plasma is switched off. It should be stressed that for each run (of which there are 11 in total), the plasma is switched on and off once. For each run, the wafers are replaced by new ones subject to the following scheme. After a dusty-plasma run, the vessel is evacuated ($<10^{-4}$ mbar) and subsequently vented with ambient air. The samples are removed after which the vessel is closed and evacuated again. For cleaning purposes, a pure oxygen plasma is run for 15 min. The oxygen line is closed and the vessel is evacuated and subsequently vented with ambient air. New samples are placed in the sample holder and the vessel is evacuated. This defines the start of a new run, and the scheme is completed again after a dusty-plasma run. The particles collected by the wafers are analyzed using SEM, and for each sample a size distribution is constructed.

In order to obtain a temporal picture of the size distribution for the dusty-plasma experiment as a whole and to correct for any run-to-run variability, the moment in time at which the plasma is switched off (τ_{off}) for each run is correlated with the first (and longest) run. This correlation is realized by synchronizing the runs to the onset of the first coagulation event (Figure 2(a)), which is the time after which the phase angle[27] increases rapidly.[25,26] This creates a common time base between all runs, which enables us to overlay τ_{off} for each run on the graph of the first and longest run, see Figure 2(b). The plasma phase angle is measured using a commercially available probe (Scientific Systems SmartPIM), placed between the matching circuit and powered electrode of the plasma. Besides the phase angle, this device measures the RF voltage, RF current, plasma-dissipated power, and plasma impedance up to the fifth harmonic at a sample frequency of 10 Hz.

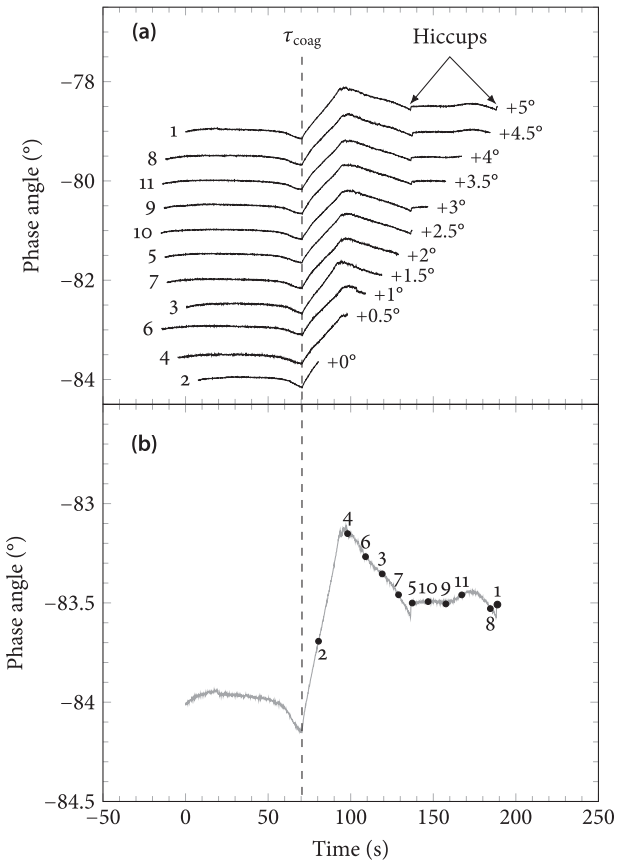

FIG. 2. (a) Phase-angle measurements of all particle-collection runs. The numbers at the left indicate the succession of the runs in reality. Each graph was shifted in the vertical direction for clarity, indicated by the numbers at the right. The discharge was switched on at the beginning of each curve and switched off at the end of each curve. The runs were synchronized with respect to the onset of coagulation τ_{coag}, which is the time after which the phase angle increases rapidly. In doing so, each run shares the same time base, meaning that the moment in time at which the plasma is switched off (τ_{off}) for each run can also be plotted on top of the graph for run 1. This is shown in (b).

For each sample, about twenty micrographs are analyzed yielding size distributions containing roughly 100 particles. Each individual micrograph is analyzed in MATLAB, which automatically detects and keeps track of circular patterns (meaning spherical particles, which was verified by analyzing tilted samples) in the micrograph, see Figure 3 for one such example.

Histograms for the samples collected below the center of the discharge and analyzed using SEM are shown in

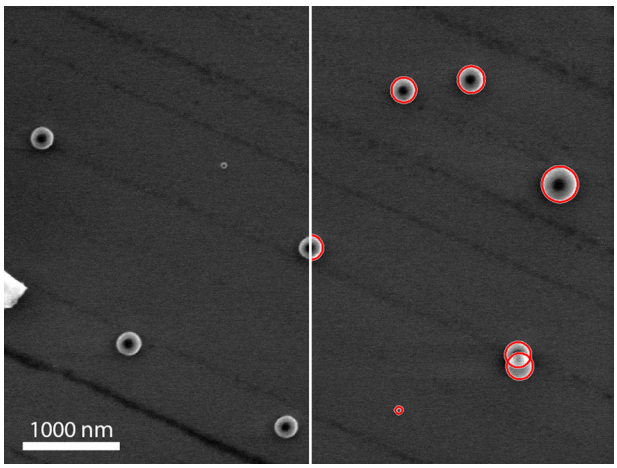

FIG. 3. A typical SEM micrograph of a small region of a single particle-collection sample. In the right half, red circles visualize the result after automatic recognition of circular patterns by the MATLAB program.

Figure 4. The histograms are shown in the order of increasing τ_{off}. A group of nucleated particles that simultaneously coagulates and subsequently grows (linearly) in time is called a "generation". Particle generations show up as clusters in a histogram. This is exactly what is observed. For example, run 2 shows one generation, run 5 shows two generations, and run 1 shows three generations. Each run corresponds to a certain moment in time at which the plasma was switched off (τ_{off}), see Figure 2. It is therefore possible to plot the mean radius of each generation as a function of this time. The result for both particle collection positions (center and edge, see Figure 1) is shown in Figure 5. The second generation becomes visible at about 137 s (directly after the first hiccup) and the third generation at the end of the graph around 188 s (directly after the second hiccup), which is direct evidence of abrupt coagulation during the void hiccups. The near-linear growth is also clearly visible, as was previously observed by, e.g., Berndt *et al.*[1] and Bouchoule and Boufendi.[11] The first generation has a radial growth rate of roughly 1.2 nm s^{-1} and the second generation of about 1.8 nm s^{-1}. It is also seen that the particle growth is virtually identical for both positions of sample collection (center and edge).

In the previous paper,[15] we showed that the void expansion speed differed between cycles. It is now possible to link this to a changed growth rate of the particles. The fact that the growth rate differs between cycles is probably related to changed ambient conditions, i.e., left-over species and changed plasma parameters. During the first growth cycle, the nanoparticles form in a relatively pristine plasma environment, whereas during any consecutive cycle, nanoparticles from previous cycles could still be present and if so are generally pushed towards the bottom of the discharge, where the sheath electric fields are able to confine them. The (former) presence of nanoparticles alters for example, the density and distribution of electrons (and their energy) and that of (metastable) atomic and molecular species; factors that all (greatly) influence growth rates.

It can be seen that the point where particles are expelled from the plasma when they reach a critical size is not yet reached for particles ending up at the silicon wafers, since this would result in a stagnated growth. This critical size is the size for which the outward-pointing forces (drag forces and/or gravity) exceed confining forces (electric field). However, no deviation from linear growth is observed within our measurement window.

A new generation of (smaller) nanoparticles appears in the SEM measurements *right after* the hiccups. Moreover, there is always one particle generation more than the number of observed void hiccups. The lower detection limit of the SEM is estimated (from the analyzed SEM images and taking into account the resolution supplied by the manufacturer) to be roughly 20 nm. Coagulated nanoparticles are expected to be at least this size. So, the fact that a new generation of nanoparticles starts to appear right after the hiccups leaves little room for alternate explanations as to what causes the void hiccup (taking into account also the MCRS and OES results published previously[15]). SEM analysis enabled us to follow the nanoparticle formation process in great detail, and it revealed clearly and directly the cyclic formation of nanoparticles in the reactive plasma.

To summarize, cyclic nanoparticle formation in a low-pressure argon-acetylene discharge was observed. Within each cycle, a dust-free zone (dust void) developed. Its expansion can be characterized by four phases: a steady expansion,

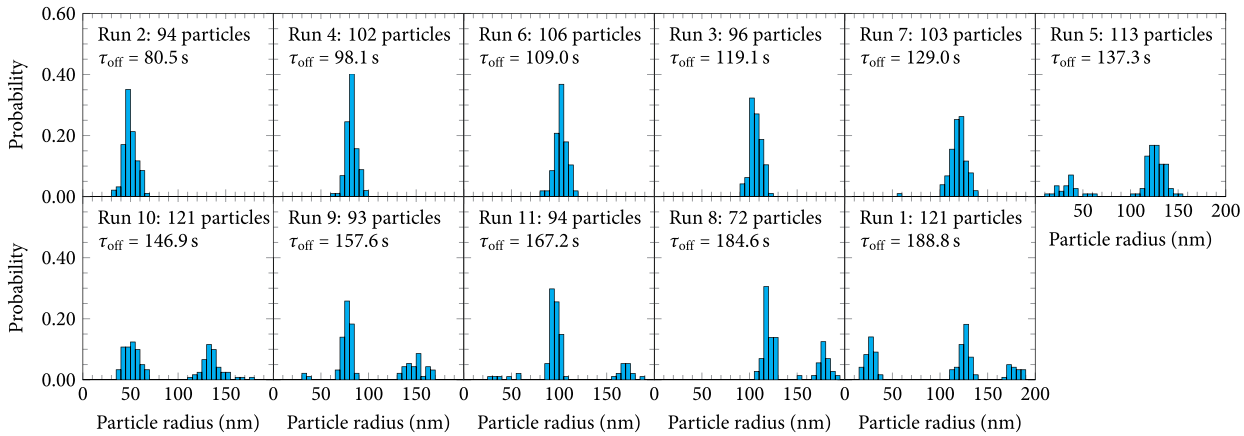

FIG. 4. Histograms of the samples collected below the center of the discharge chamber for the runs as in Figure 2. The number of particles in each histogram is also listed. The moment in time at which the plasma was switched off (τ_{off}) increases from left to right in each row.

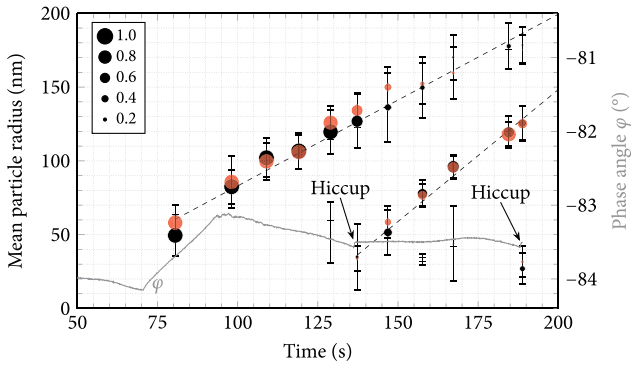

FIG. 5. Mean particle radius for each generation as a function of time for particles collected directly below the center (black) and near the edge of the discharge chamber (red). The size of the dots indicates the fraction of that generation within an individual sample. Error bars signify two sample standard deviations. The plasma phase angle is plotted in gray for reference.

a rapid expansion, a contraction (termed "hiccup"), and finally a continued expansion.

The void hiccup is caused by a sudden coagulation of nucleated nanoparticles within the expanding void. Direct experimental proof is given for the localized coagulation of nanoparticles in the void by employing a multitude of diagnostics. This letter presents the analysis of particles collected at different moments in time spanning several growth cycles using scanning electron microscopy. The SEM analysis provides a direct insight into the cyclic formation of nanoparticles in the reactive plasma and leaves little room for alternate explanations – other than an abrupt coagulation – causing the void hiccup.

The authors wish to thank Ab Schrader, Eddie van Veldhuizen and Luc Stevens for their skillful technical support. This work was supported by NanoNextNL, a micro and nanotechnology programme of the Dutch Government and 130 partners.

[1]J. Berndt, E. Kovačević, I. Stefanović, O. Stepanović, S. H. Hong, L. Boufendi, and J. Winter, Contrib. Plasma Phys. **49**, 107 (2009).
[2]J. Berndt, H. Acid, E. Kovacevic, C. Cachoncinlle, T. Strunskus, and L. Boufendi, J. Appl. Phys. **113**, 063302 (2013).
[3]A. Kuzminova, A. Shelemin, O. Kylián, M. Petr, J. Kratochvíl, P. Solař, and H. Biederman, Vacuum **110**, 58 (2014).
[4]U. Kortshagen, J. Phys. D: Appl. Phys. **42**, 113001 (2009).
[5]K. G. Spears, T. J. Robinson, and R. M. Roth, IEEE Trans. Plasma Sci. **14**, 179 (1986).
[6]G. S. Selwyn, J. Singh, and R. S. Bennett, J. Vacuum Sci. Technol. A **7**, 2758 (1989).
[7]J. Winter, Plasma Phys. Controlled Fusion **40**, 1201 (1998).
[8]J. Winter, Plasma Phys. Controlled Fusion **46**, B583 (2004).
[9]S. Wurm, Proc. SPIE **9231**, 923103 (2014).
[10]L. Boufendi and A. Bouchoule, Plasma Sources Sci. Technol. **3**, 262 (1994).
[11]A. Bouchoule and L. Boufendi, Plasma Sources Sci. Technol. **2**, 204 (1993).
[12]L. Boufendi, J. Hermann, A. Bouchoule, B. Dubreuil, E. Stoffels, W. W. Stoffels, and M. L. de Giorgi, J. Appl. Phys. **76**, 148 (1994).
[13]E. Kovacevic, J. Berndt, T. Strunskus, and L. Boufendi, J. Appl. Phys. **112**, 013303 (2012).
[14]C. Hollenstein, W. Schwarzenbach, A. A. Howling, C. Courteille, J.-L. Dorier, and L. Sansonnens, J. Vacuum Sci. Technol. A **14**, 535 (1996).
[15]F. M. J. H. van de Wetering, R. J. C. Brooimans, S. Nijdam, J. Beckers, and G. M. W. Kroesen, J. Phys. D: Appl. Phys. **48**, 035204 (2015).
[16]M. Cavarroc, M. Mikikian, Y. Tessier, and L. Boufendi, Phys. Rev. Lett. **100**, 045001 (2008).
[17]J.-C. Schauer, S. Hong, and J. Winter, Plasma Sources Sci. Technol. **13**, 636 (2004).
[18]I. Stefanović, C. Scharwitz, E. Kovačević, J. Berndt, and J. Winter, IEEE Trans. Plasma Sci. **36**, 1018 (2008).
[19]S. Hong, J. Berndt, and J. Winter, Plasma Sources Sci. Technol. **12**, 46 (2003).
[20]D. Samsonov and J. Goree, Phys. Rev. E **59**, 1047 (1999).
[21]J. Goree, G. E. Morfill, V. N. Tsytovich, and S. V. Vladimirov, Phys. Rev. E **59**, 7055 (1999).
[22]V. Land and W. J. Goedheer, New J. Phys. **9**, 246 (2007).
[23]M. Y. Pustylnik, A. V. Ivlev, N. Sadeghi, R. Heidemann, S. Mitic, H. M. Thomas, and G. E. Morfill, Phys. Plasmas **19**, 103701 (2012).
[24]M. Schulze, A. von Keudell, and P. Awakowicz, Plasma Sources Sci. Technol. **15**, 556 (2006).
[25]J. Beckers, "Dust particle(s) (as) diagnostics in plasmas," Ph.D. thesis, Eindhoven University of Technology (2011).
[26]J. Beckers and G. M. W. Kroesen, Appl. Phys. Lett. **99**, 181503 (2011).
[27]The plasma phase angle is the phase difference between the voltage over the discharge and the current flowing through it. The nanoparticle formation process can be followed by inspecting the plasma phase angle, since nanoparticles present resistive losses in a plasma, meaning that during their growth they will increase the phase angle from values close to −90° (ideal capacitor) to closer to zero.